

DSC-MRI Derived T2* Leakage Effect Depends on Structural Features of Extravascular Space

Natnael B Semmineh¹, Junzhong Xu¹, Jerry Boxerman², Gary W. Delaney³, and C. Chad Quarles¹

¹Institute of Imaging Science, Vanderbilt University, Nashville, TN, United States, ²Alpert Medical School of Brown University, Providence, Rhode Island, United States, ³CSIRO Mathematical and Information Sciences, Clayton South, Vic, Australia

Target Audience: Clinicians and basic scientists who apply and investigate DSC-MRI methods in patients with brain tumors.

Purpose: In DSC-MRI studies, the leakage of contrast agent (CA) into the extravascular extracellular space (EES) creates magnetic susceptibility differences ($\Delta\chi$) between cells and the EES, which can result in additional extravascular T_2^* effects well after the initial bolus of CA passes through the tissue. These effects have been clinically assessed using such metrics as the percent signal recovery [1]. Such DSC-MRI signals are influenced by the extravascular compartmentalization of CA and could potentially be used to extract information about the underlying cellular properties within tissue (e.g. cell density, intercellular distance) [2]. The goals of this study were to investigate the relationship between the extravascular T_2^* effects and the complex cellular properties in tumors.

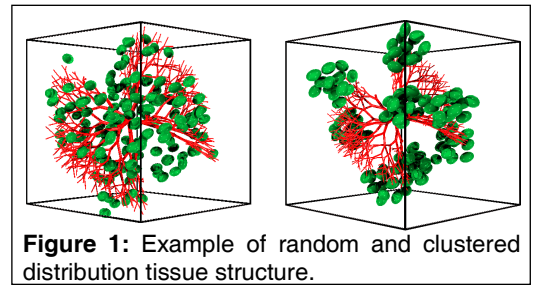


Figure 1: Example of random and clustered distribution tissue structure.

Methods: To investigate the dependence of extravascular T_2^* effects on cellular features, we simulated 3D tissue structures using fractal tree based vascular network and randomly distributed ellipsoids. For each set of phantoms we varied the extravascular features such as, cell volume fraction, cellular cluster volume and inter cellular separation, while keeping a fixed vascular network of 2.5% volume fraction. Magnetic field perturbations induced by susceptibility variations between the simulated tissue compartments, and the associated gradient echo transverse relaxation rates, were computed using the Finite Perturber Finite Difference Method (FPFDM) [3]. We specifically considered the case when the susceptibility based contrast contribution from the vasculature is substantially lower than that during the first pass, which corresponds to several minutes after an injection of a small molecular weight CA. The slope of the computed ΔR_2^* versus tissue CA concentration ($[CA]_t$) was used to estimate a coefficient termed the tissue cellularity index (TCI). Assuming that the CA does not penetrate into the intracellular space, the tissue CA concentration is calculated as the sum of intravascular and EES CA concentrations weight by the respective volume fractions.

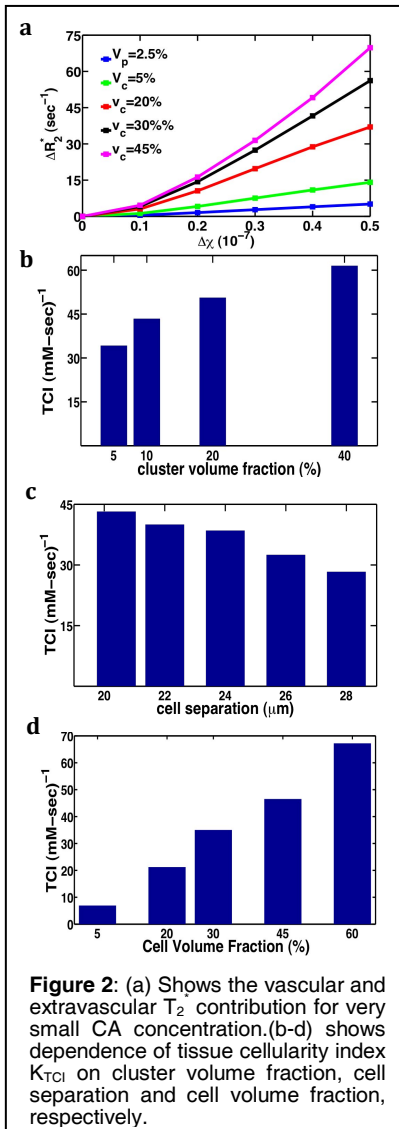


Figure 2: (a) Shows the vascular and extravascular T_2^* contribution for very small CA concentration. (b-d) shows dependence of tissue cellularity index K_{TCI} on cluster volume fraction, cell separation and cell volume fraction, respectively.

Results: Figure 1 shows example tissue structures created using fractal based vascular tree network along with randomly distributed and disordered clusters of ellipsoids. For very small intravascular and EES CA concentration, long after the first bolus pass, the computed tissue ΔR_2^* value is dominated by the extravascular T_2^* effects as shown in Fig. 2a. The results in Fig. 2a are computed for four extravascular tissue structures with cellular volume fraction ranging from 5% to 45%, and one vascular tree network with a volume fraction of 2.5%. For a susceptibility value corresponding to one fifth of the peak susceptibility variation created by a typical DSC-MRI bolus injection there is 90.5% difference between the ΔR_2^* values computed for the vascular structure contribution and extravascular structure of 45% cell volume fraction. Fig. 2b shows TCI values for tissue structures simulated using small to large cellular cluster distribution. For a fixed total cell volume fraction of 40% increasing the cluster volume from 5% to 40% results in a two fold increase in TCI. The dependence of TCI on cellular separation is shown in Fig. 2c. For a fixed cell volume fraction of 30% increasing the intercellular separation from 20-28 μm , about the size of the average radii of the ellipsoids, the TCI decreases by 34%. Fig. 2d shows the high sensitivity of TCI to changes in cell volume fraction. An increase in cell volume fraction from 45% to 60% yields a 30% increase in TCI.

Discussion: As indicated in Figure 2a, the influence of tissue cellularity on DSC-MRI derived ΔR_2^* values, at time points where the CA concentration in the intra- and extra-vascular space is similar, is higher than the vascular contribution. We are currently computing this relationship for higher vascular volume fractions. The observation that ΔR_2^* values increase with increasing cell cluster volume and decreases with intercellular separation indicates that CA compartmentalization within clusters of compact cellular distributions increases field perturbation heterogeneity. Given the sensitivity of DSC-MRI data acquired for several minutes after the first pass indicates that this approach may be a new imaging method to probe tumor cellularity, as we recently proposed [4,5,6].

Conclusion: Taken together these results demonstrate that DSC-MRI data acquired in the presence of CA leakage is highly dependent on cellular clustering, density and spatial distribution. This finding suggests that such DSC-MRI data could potentially be used to extract biomarkers of tumor cellular properties and be used to evaluate treatment response. The magnitude of these effects during the first pass, and their influence on the computed blood flow and blood volume parameters, is currently under investigation.

References: [1] R. Mangla, et al, AJNR Am J Neuroradiol, 2010. [2] Quarles CC, et al, Phys Med Biol, 2009. [3] Semmineh N., et al. ISMRM 2011 p. 3918. [4] Semmineh N., et al. ISMRM 2012 p. 1956. [5] Semmineh N., et al. ISMRM 2012 p. 1526. [6] Semmineh N., et al. ISMRM perfusion MRI 2012.

Acknowledgements: NCI R00 CA127599, NCI R01 CA158079, NCI P30 CA068485, NCI U24 CA126588